Available online at www.sciencedirect.com
SCIENCE DIRECT®
Journal of Molecular Catalysis A: Chemical 215 (2004) 137–142
JOURNAL OF MOLECULAR CATALYSIS A: CHEMICAL
www.elsevier.com/locate/molcata

Preparation and photocatalytic properties of Zr^{4+}-doped TiO_2 nanocrystals

Yan Min Wang [a], Su Wen Liu [a,b,*], Meng Kai Lü [b], Shu Fen Wang [b], Feng Gu [b], Xue Zhou Gai [a], Xiao Peng Cui [a], Jie Pan [a]

[a] *Material Science and Engineering Department, Shangdong Institute of Light Industry, Jinan 250100, PR China*
[b] *State Key Laboratory of Crystal Material, Shandong University, Jinan 250100, PR China*

Received 11 November 2003; received in revised form 5 January 2004; accepted 11 January 2004

Abstract

Zirconium ions (Zr^{4+})-doped titanium dioxide (TiO_2) nanocrystal was prepared by sol–gel method. The structure and surface morphology of the samples were characterized by X-ray diffraction (XRD), infra-red (IR) spectra and transmission electron microscopy (TEM), and moreover the specific surface area of the samples was investigated by Brunauer–Emett–Teller (BET) method. The photocatalytic efficiency and the anti-inactivation stability of pure and doped TiO_2 was tested by decolorizing methyl orange and degrading nitrobenzene solution. The results showed that low-amount presence of Zr^{4+} could suppress the growth of TiO_2 grains, raise the surface area, and accelerate surface hydroxylation, which resulted in the higher photocatalytic activity of the doped TiO_2. The first degradation results of doped samples were all higher than pure TiO_2 and TiO_2 Degussa P_{25}, and when the Zr^{4+} content was 6 mol%, the photocatalytic efficiency of $Ti_{0.94}Zr_{0.06}O_2$ was 1.5 times as high as that of pure TiO_2 investigated by spectrophotometry and gas chromatography; however the Degussa P_{25} presented the highest anti-inactivation stability.
© 2004 Elsevier B.V. All rights reserved.

Keywords: TiO_2; Sol–gel; Zirconic doped; Photocatalysis

1. Introduction

Nanometer scaled TiO_2 is a quite stable photocatalyst with the virtues of nonpoisonous, cheap, easy obtainment, etc. In addition, TiO_2 photocatalyst has the functions of sterilize, desodoration, surface self-cleaned. So, it is used extensively in the air purification and sewage treatment fields [1–3]. However, because of its big forbidden band only ultraviolet with the energy of more than 3.2 eV can stimulate its photocatalytic action, which limits its applicability to great extent. In order to enhance its applicability and photocatalytic property, undoubtedly, ion doping and composite semiconductors are important measures. ZrO_2 is an important material widely used in ceramics technology [4] and in heterogeneous catalysis [5,6]. TiO_2 and ZrO_2 are both n-type semiconductors. So, in recent years TiO_2–ZrO_2 system used as potential photocatalyst has been reported [7,8] and the solid solution $ZrTiO_4$ was obtained successfully at low temperature [9,10]. But little attention was paid to Zr^{4+}-doped TiO_2 used as photocatalyst.

In this paper, Zr^{4+}-doped TiO_2 nanocrystal was prepared by sol–gel method and Zr^{4+} was introduced in the form of inorganic salt $ZrOCl_2$. And the photocatalytic efficiency of the samples was investigated by spectrophotometry and gas chromatography. At the same time, by analysing its structure and surface morphology the effects of Zr^{4+} on photocatalysis properties were studied.

2. Experimental

Samples of Zr^{4+} doped TiO_2 were prepared by sol–gel method using $Ti(OC_4H_9)_4$ (C.R), $ZrOCl_2$(C.R) as raw materials and hydrochloric acid (HCl A.R) as catalyst. The TiO_2 sol was obtained by the following: $Ti(OC_4H_9)_4$ was dissolved in C_2H_5OH (about 2/3 vol.) forming the solution of precursor. Secondly, the mixture of C_2H_5OH (about 1/3 vol.), HCl and H_2O was mixed dropwise into the precursor solution under magnetic stirring. The molar ratio

* Corresponding author. Tel.: +86-5318605148; fax: +86-5318619798.
E-mail address: swliu@icm.sdu.edu.cn (S.W. Liu).

1381-1169/$ – see front matter © 2004 Elsevier B.V. All rights reserved.
doi:10.1016/j.molcata.2004.01.007

of $Ti(OC_4H_9)_4$:C_2H_5OH:H_2O:HCl was 1:20:1:0.1. At the same time, $ZrOCl_2$ was decentralized in C_2H_5OH and H_2O was mixed dropwise into the suspension according to the molar ratio of $ZrOCl_2$:C_2H_5OH:H_2O (1:40:5). The ZrO_2 sol was also obtained. Finally, adding ZrO_2 sol to TiO_2 sol the mixing sol was obtained after 3 h stirring at room temperature. The sol could solidify after about 24 h aging, and after 5 h drying at 100 °C the xerogels were obtained. Then the xerogels were annealed at 500 °C for 15 min and the pure and doped TiO_2 powders were obtained after grinding. The doping molar ratio of Zr^{4+} was x ($x = 0$, 0.02, 0.04, 0.06, 0.08, 0.10, 0.12) and the correspondent samples were expressed as $Ti_{1-x}Zr_xO_2$.

The crystalline structure of the samples annealed at 500 °C for 15 min was investigated by XRD on Japan RigaKu D/MAX 2200PC diffractometer with Cu Kα radiation ($\lambda = 0.15418$ nm) and graphite monochromator. Transmission electron microscopy (TEM) was carried out on a TEM-100CXII transition electron microscope. The IR spectra were carried out on NEXUS 670 FT-IR instrument. The specific surface area was investigated by Brunauer–Emett–Teller (BET) method on ST-08A metering equipment.

First, the photocatalysis property and anti-activity stability were investigated by decolorizing methyl orange under the illumination of 20 W/220 V UV lamp for 0.5 h. The amount of catalyst used was 3 g/l, the illumination distance was 8 cm, the initial concentration and the pH value of methyl orange solution were 20 mg/l and 5.8, respectively. In order to investigate the catalysts' anti-inactivation stability, the degraded suspension was centrifugally separated on LG10-2.4A centrifugation instrument; afterwards the precipitated catalyst was washed by distilled water for several times and the dried catalyst was used repeatedly. The absorbance of the methyl orange solution was investigated on a U-3500 Spectrophotometer at a wavelength of 465 nm. The discoloration ratio (η) and the concentration (C) of the degraded methyl orange solution could be obtained according to [11] and the results were shown in Table 2. Afterwards, in order to verify their photoactivity, we degraded nitrobenzene solution. The illuminant, the amount of catalyst used and the illumination distance were same to methyl orange solution; the initial concentration and the pH value of nitrobenzene solution were 20 mg/l and 5.1, respectively. The concentration (C) and the degradation rate (η) of the nitrobenzene were detected by SP-6800 gas chromatography.

3. Results and discussion

From the XRD patterns of the samples annealed at 500 °C (shown in Fig. 1), all the diffraction lines are assigned to tetrahedral configuration anatase and there are no diffraction lines of new phases of $ZrTiO_4$ and ZrO_2. According to the Scherrer equation ($d = k\lambda/\beta\cos\theta$), we can evaluate the grain size (the grain size of pure TiO_2, $Ti_{0.94}Zr_{0.06}O_2$ and $Ti_{0.88}Zr_{0.12}O_2$ are 13.3, 10.3 and 11.4 nm, respectively), which show the doping of the Zr^{4+} can suppress the grain growth and lead to the smaller grain size. Comparing to that of pure TiO_2 broadened diffraction peaks and diffraction Bragg angles moving to low-angle range can also be observed, that is to say, the introduction of Zr^{4+} contributes to the lattice deformation.

TEM micrographs of pure TiO_2 and $Ti_{0.94}Zr_{0.06}O_2$ annealed at 500 °C for 15 min are shown in Fig. 2. It is observed that the nanoparticles are spherical and grain agglomeration appears. According to the micrographs, the grain size can also be estimated (the average grain size of pure TiO_2 and $Ti_{0.94}Zr_{0.06}O_2$ is 14 and 10 nm, respectively), which is consistent with the XRD results.

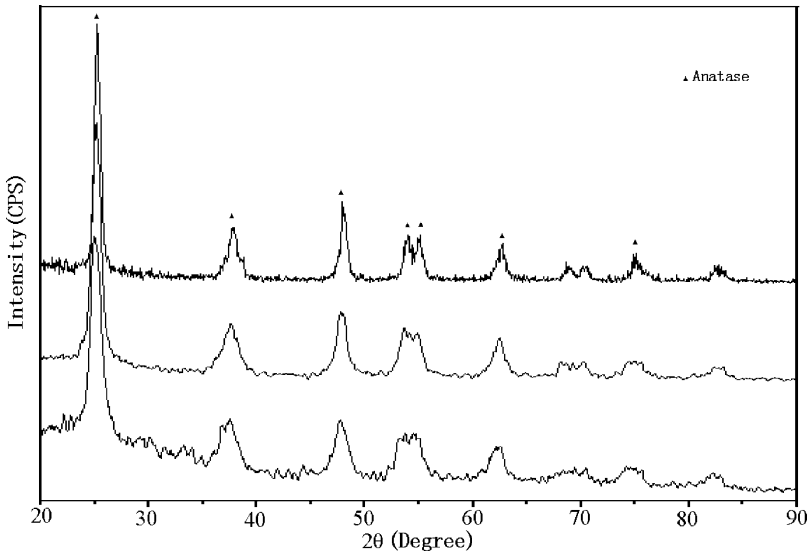

Fig. 1. The XRD patterns of the samples annealed at 500 °C for 15 min: (a) pure TiO_2; (b) $Ti_{0.94}Zr_{0.06}O_2$; and (c) $Ti_{0.88}Zr_{0.12}O_2$.

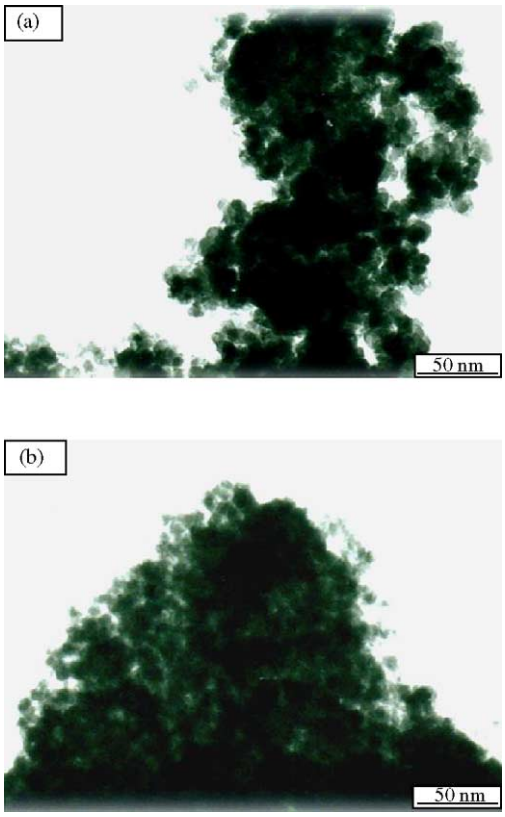

Fig. 2. TEM micrograph of the samples annealed at 500 °C for 15 min: (a) pure TiO_2; and (b) $Ti_{0.94}Zr_{0.06}O_2$.

Fig. 3 shows IR spectra of TiO_2, $Ti_{0.94}Zr_{0.06}O_2$ and $Ti_{0.94}Zr_{0.06}O_2$ powder heat-treated at 500 °C for 15 min. In all spectra, bands appear at around 3384, 2920, 2850, and 1620 cm^{-1}. The bands at 3384 and 1620 cm^{-1} represent the stretching and bending vibrations of O–H bond, and in Fig. 3b the adsorption intensity strengthens obviously implying the surface hydroxyl amount of $Ti_{0.94}Zr_{0.06}O_2$ is higher than the other samples [12]. The bands at 2920 and 2850 cm^{-1} are due to the C–H bonds of the organic compounds. The absorption peaks in the range of 1300–1500 cm^{-1} are the vibrational fingerprint lines of organic bond. In Fig. 3b and c, the band around 2970 cm^{-1} represents the stretching vibrations of H–Cl bond and no band appears in Fig. 3a at around 2970 cm^{-1}, which are due to Zr^{4+} ions introduced by $ZrOCl_2$ bringing more Cl^- to the sample. In the range of 400–700 cm^{-1}, the adsorption band broadens into a absorption terrace. There are two reasons for the terrace. Firstly, the dimension of the grains distributed in a range can result in the different surface tension and the different lattice deformation. So, the bond length has a distribution range. In addition, the interface volume of nanomaterial holds a big ratio and the bond of inner is different from that of interface for the surface atoms coordination number is inadequate [13].

Table 1
The surface area of different samples

x (Zr^{4+} mol%)	S_{BET} (m^2/g)
0	35.4941
0.02	65.8654
0.04	74.9432
0.06	84.6582
0.08	87.1300
0.10	90.4418
0.12	93.7712
P_{25}	47.4502

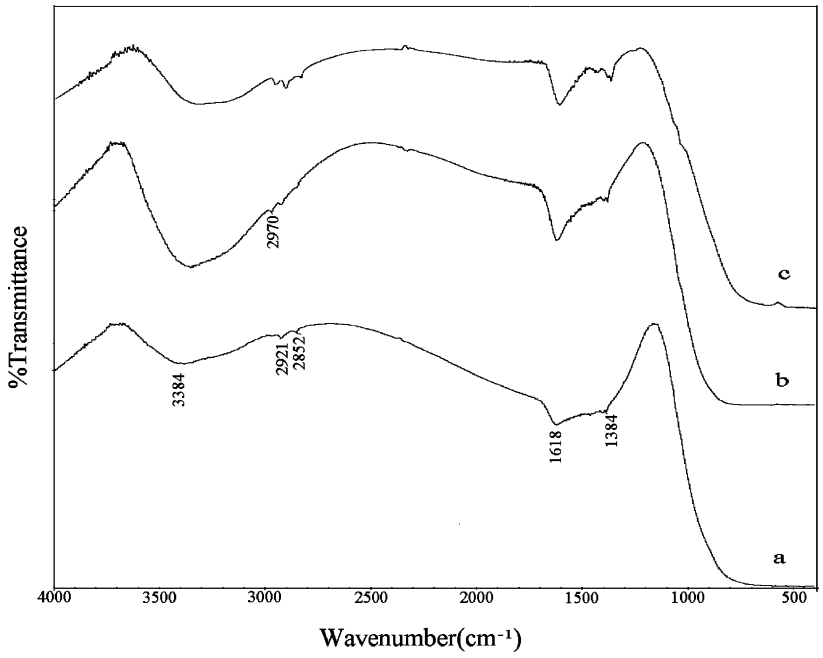

Fig. 3. The FT-IR spectra of the samples annealed at 500 °C for 15 min: (a) pure TiO_2; (b) $Ti_{0.94}Zr_{0.06}O_2$; and (c) $Ti_{0.88}Zr_{0.12}O_2$.

Table 2
The testing results of decolorizing methyl orange

	x (Zr^{4+} mol%)							
	0.00	0.02	0.04	0.06	0.08	0.10	0.12	P_{25}
η_1 (%)	50.53	77.64	78.20	87.70	81.4	76.3	70.16	57.21
η_2 (%)	61.7	52.9	62.9	67.8	66.4	59.5	56.6	46.2
η_3 (%)	24.8	14.4	27.3	32.2	23.9	16.9	14.2	39.6
η_4 (%)	13.9	12.0	24.4	25.4	23.4	15.6	8.1	35.1

Notes: η_1, η_2, η_3 and η_4, respectively, represent the first, second, third and the fourth decolorizing rate of methyl orange.

For a better explanation of the photocatalytic results, the specific surface area of the samples was investigated and the values are listed in Table 1. From Table 1, the values of doped samples are obviously higher than that of pure TiO_2 and Degussa P_{25} and they increase with the increasing amount of Zr^{4+} ion, and furthermore when the Zr^{4+} content was 12 mol%, the value of $Ti_{0.88}Zr_{0.12}O_2$ is 2.6 times as high as that of pure TiO_2 and two times as high as that of Degussa P_{25}. This shows that the presence of Zr^{4+} can obviously raise the surface area of the samples.

The results of decolorizing methyl orange are shown in Table 2. From Table 2, we can see that the decolorizing ratio of the doped powders is not only higher than that of the pure TiO_2, but also higher than that of Degussa P_{25}. The decolorizing ratio increases and then decreases with the increasing amount of Zr^{4+} ions. When the Zr^{4+} content is 6 mol% the decolorizing ratio of the samples is the highest. We can also observe that decolorizing ratio decreases with the increasing of used times, that is, $\eta_1 > \eta_2 > \eta_3 > \eta_4$. In order to verify its changing tendency, we select the representative results of TiO_2, $Ti_{0.94}Zr_{0.06}O_2$, $Ti_{0.88}Zr_{0.12}O_2$, P_{25} to plot between the used times and discoloration ratio (Fig. 4). From Fig. 4, we can observe when the samples have been used two times their photoactivity decreases. By comparing the decreasing tendency, we can conclude the following anti-inactivation stability order: $P_{25} \gg TiO_2 > Ti_{0.94}Zr_{0.06}O_2 > Ti_{0.88}Zr_{0.12}O_2$. The anti-inactivation stability of $Ti_{0.88}Zr_{0.12}O_2$ is the poorest, and that of Degussa P_{25} is the best. This can be ascribed to the bigger surface area of the doped samples, which have bigger adsorption ability to the smaller molecules compared to pure TiO_2. And as a result most of the active positions are blocked [14].

Table 3 shows the degradation results investigated by gas chromatography and Fig. 5 are the representative gas chromatography spectra of the nitrobenzene solution. From Fig. 5 and Table 3, we can observe the changes of the peak area, the degradation ratio (η) and the solution concentration (C), implying the photocatalysis activity of the samples. We can see that η_c is about 1.5 times of η_b, that is to say, the photocatalytic activity of $Ti_{0.94}Zr_{0.06}O_2$ is 0.5 times higher than that of pure TiO_2 at the same condition.

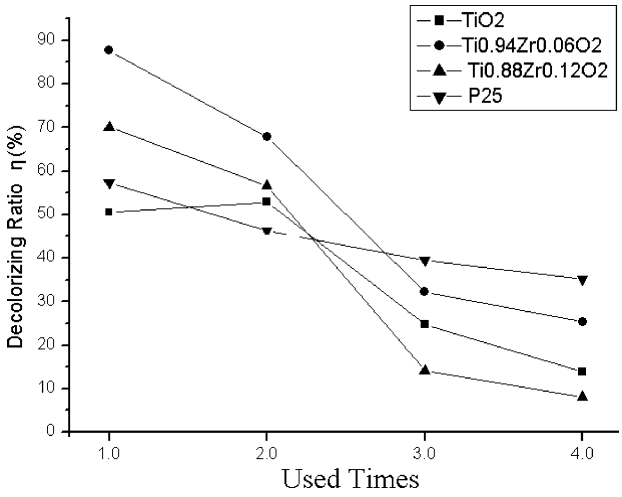

Fig. 4. The curves between used times and decolorizing ratio.

The photocatalytic efficiency depends on the ratio of the photo-generated surface carriers transfer rate to the electron–hole (e^-/h^+) recombination [1,15]. The increased photocatalytic activity of the doped powders has three aspects. Firstly, according to the diffusing equation, $\tau = r/\pi^2 D$ (τ represents the average diffusing time, r the grain size and D the diffusing coefficient of carriers), the average diffusing time is in direct proportion to the grain size. As such, the smaller grain size contributes to the shorter diffusing time of the photo-generated carriers from the inner to the surface. In addition, research displays that the electron and hole can be captured speedily [16]. Therefore, the smaller grain size can enhance separation efficiency and cut down the combination efficiency of the photo-generated electric charge. Secondly, Zr^{4+} is isoelectronic impurity and belongs to deep energy level doping [17]. So, the main function of Zr^{4+} doped is forming the traps, which can trap electrons or holes to suppress the combination of e^-/h^+. According to the equation [18], $K_{combination} \propto \exp(-2R/a_0)$ (K represents the combination velocity, R the distance of separating electron and

Table 3
The degradation results of nitrobenzene investigated by gas chromatography

	x (Zr^{4+} mol%)								
	0.00	0.02	0.04	0.06	0.08	0.10	0.12	P_{25}	Standard solution
Retention time (min)	0.710	0.715	0.718	0.720	0.717	0.715	0.712	0.714	0.713
Peak area	2003	1833	1812	1777	1798	1844	1902	1932	2421
C (mg/l)	16.5	15.1	15.0	14.7	14.9	15.2	15.7	16.0	20.0
η (%)	17.3	24.3	25.2	26.6	25.7	23.8	21.4	19.9	–

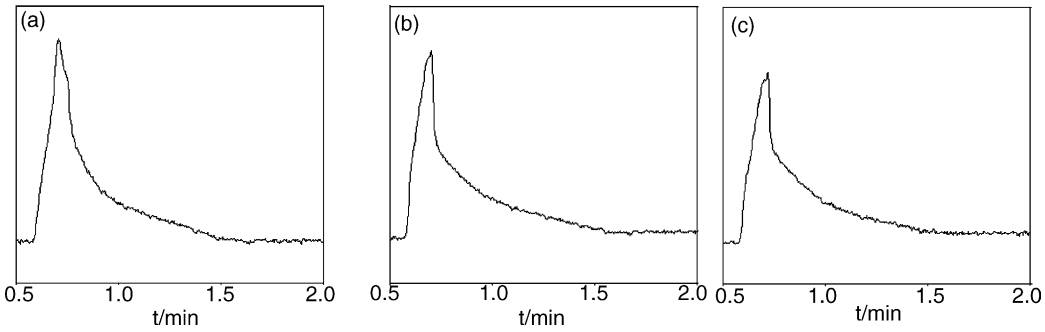

Fig. 5. Gas chromatograms of the nitrobenzene solution: (a) the standard solution; (b) the solution degraded 2 h by pure TiO_2; and (c) the solution degraded 2 h by $Ti_{0.94}Zr_{0.06}O_2$. Chromatographic conditions: FID detection; carrier gas: N_2; injection amount: 1 μl; and column temperature: 190 °C.

hole, and a_0 the resembling hydrogen wave equation radius of the capture carriers), the velocity of e^-/h^+ combination is determined by the distance of separating electron and hole (that is the so-called average distance between capture traps). Therefore, when the doped concentration is less than the optimum value, there are no enough traps to capture the charge carriers. And when the concentration is more than the optimum value (in this paper is 6%), the smaller R can result in the exponential growth of $K_{combination}$. Thirdly, according to the IR spectra the surface hydroxyl amount of $Ti_{0.94}Zr_{0.06}O_2$ is the highest, which is not only favor for the trapping of electrons to enhance the separation efficiency of electron-hole pair, but also favor for the forming of surface free radical ($^{\bullet}OH$) to oxidize the contaminants. So, the photocatalytic activity of $Ti_{0.94}Zr_{0.06}O_2$ is the highest.

In addition, possessing bigger surface area is one of the basic terms of catalysts. Under normal conditions, the concentration of pollutants is very low, so the assembling concentration around TiO_2 is low. At the same time, the photo-oxidation process of TiO_2 must be carried out on its surface, so it will take long time to accomplish the photocatalytic reaction and the photocatalytic efficiency is very low. Therefore, the doped samples with bigger surface area have higher adsorption ability to the pollutants, which can contribute to the higher photocatalytic ability. However, if the adsorption ability of carriers is too high and although it can adsorb much more pollutants, it does not profit the diffusing of pollutants to TiO_2 surface [19,20]. Although ZrO_2 possesses good absorptive properties [21], in this paper the absorptive properties of home-prepared nanocrystals are poor because of the low doped-content and the bigger molecule of methyl orange. Therefore, the "additional" decolorizing rate is very small resulting from adsorption (in the experiment, we have subtracted it by investigating the pre- and post-irradiation absorbance of the solution).

Generally speaking, the factors that affect the photocatalytic efficiency also include illuminant and light intensity, the solution pH, inorganic salts, additional oxidizer, reaction temperature and so on, besides the catalyst-self factors (such as crystalline phase, grain size, surface area and surface hydroxyl). It has been reported [22,23] that the changing of pH value has different influence on different pollutants, and Harada [24] has investigated the influence of light intensity on quantum yield under different pH value. In this paper, we have controlled the pH value of the methyl orange and nitrobenzene solution to be 5.8 and 5.1, respectively.

4. Conclusion

Zr^{4+}-doped TiO_2 nanopowder with higher photocatalytic activity has been successfully prepared by sol–gel method. The photocatalytic activity of the doped samples is higher than that of pure TiO_2, when the content of Zr^{4+} is 6 mol%, the photocatalytic efficiency of the sample is 1.5 as high as that of pure TiO_2. The introducing of Zr^{4+} leads to smaller grain size, bigger surface area, larger lattice deformation and the forming of capture traps, which contribute to the higher separation efficiency of the photogenerated carriers. However, the anti-inactivation stability of doped samples is poorer, and that of Degussa P_{25} is better. This can be ascribed to the bigger surface area of the doped samples, which have bigger adsorption ability to the small molecules comparison to pure TiO_2 and Degussa P_{25}. And as a result most of the active positions are blocked when the doped samples are used continuously.

Acknowledgements

The author thanks the Natural Science Foundation of Shangdong Province for support. The number is Y2000F04.

References

[1] J.C. Yu, J. Yu, W. Ho, Z. Jiang, L. Zhang, Chem. Mater. 14 (2002) 3808.
[2] A. Peiró, J. Peral, C. Domingo, X. Domènech, J. Ayllón, Chem. Mater. 13 (2001) 2567.
[3] A. Yasumori, H. Shinoda, Y. Kameshima, S. Hayashi, K. Okada, J. Mater. Chem. 11 (2001) 1253.
[4] D.A. Ward, E.I. Ko, Chem. Mater. 5 (1993) 956.
[5] H.H. Kung, Transition metal oxides, surface chemistry and catalysis, Stud. Surf. Sci. Catal. 45 (1989) 721.

[6] A. Corma, Chem. Rev. 95 (1995) 559.
[7] G. Colón, M. Hidalgo, J. Navío, Appl. Catal. A: Gen. 231 (2001) 185.
[8] M. Zorn, D. Tompkins, W. Zeltner, M. Anderson, Appl. Catal. B: Environ. 23 (1999) 1.
[9] J.A. Navio, F.J. Marchena, M. Macias, P.J. Sanchez-Soto, P. Pichat, J. Mater. Sci. 27 (1992) 2463.
[10] J. Fung, I. Wang, J. Catal. 130 (1991) 577.
[11] S.W. Liu, C.F. Song, M.K. Lü, S.F. Wang, D.L. Sun, Y.X. Qi, D. Xu, D.R. Yuan, Catal. Commun. 4 (2003) 343.
[12] F. Babou, G. Coudurier, J. Vedrine, J. Catal. 152 (1995) 341.
[13] L.D. Zhang, C.M. Mo, T. Wang, Phys. Status Solidi A 136 (1993) 291.
[14] A. Huang, L. Cao, J. Chen, J. Catal. 188 (1999) 40–47.
[15] Y. Jiaguo, Z. Qingnan, Mater. Chem. Phys. 69 (2001) 25.
[16] G. Rothenberger, J. Moser, M. Gratzel, J. Am. Chem. Soc. 107 (1985) 8054.
[17] S.T. Pantelides, Rev. Mod. Phys. 50 (1978) 797.
[18] M. Gratzel, Heterogenerous Photochemical Electron Transfer, CRC Press, Boca Raton, FL, 1989.
[19] N. Takeda, M. Dhtani, J. Physchem. 101 (1997) 2644.
[20] N. Takeda, N. Iwata, J. Catal. 177 (1998) 240.
[21] J.A. Navio, G. Colón, J.M. Herrmann, J. Photochem. Photobiol. A: Chem. 108 (1997) 185–197.
[22] A.L. Pruden, D.F. Ollis, Environ. Sci. Technol. 17 (1983) 628–631.
[23] H. Harada, T. Ueda, T. Sakata, J. Phys. Chem. 93 (1989) 1542–1548.
[24] H. Harada, T. Ueda, Chem. Phys. Lett. 106 (1984) 229–231.